Improving Ionospheric determinations at UPC: Kriging and Wide Area RTK techniques

R.Orus, M.Hernández-Pajares, J.M. Juan, J.Sanz,
gAGE/UPC, Research group of Astronomy and Geomatics
Technical University of Catalonia
Barcelona, Spain
Contact e-mails: rorus@mat.upc.es, manuel@mat.upc.es

Abstract

The purpose of this talk is to summarize the last results obtained at UPC, in two problems, which suppose a significant improvement of the corresponding ionospheric determinations:

1) The application of a Kriging interpolation technique adapted to the global Total Electron Content mapping, especially useful in the context of the IGS reprocessing campaign.

2) The improvement of the Wide Area Real Time Kinematics (WARTK) technique (originally based on an optimal combination of a real-time precise ionospheric and geodetic modelling) with a simple Medium Scale Travelling Ionospheric Disturbance (MSTID) modelling.

Indeed, the Kriging technique has shown its potential in order to significantly improve the performance of the ionospheric interpolation, being an important point in global TEC mapping, due to the lack of receivers in large areas over the Seas and South Hemisphere (see for example Orus et al. 2005). The reason behind such improvement is that Kriging takes optimally into account the spatial error decorrelation.

An other ionospheric front in which significant improvements have been achieved recently corresponds to high accuracy ionospheric corrections, supporting cm-error-level GNSS navigation at continental scales, based for example on the Satellite Based Augmentation reference receivers, SBAS systems, such as the EGNOS RIMS (see Hernández-Pajares et al. 2002).

Indeed, in order to achieve cm-error-level navigation, is important to correctly estimate the carrier phase ambiguities. In this context, the WARTK technique allows such fixing in baselines up to hundreds of km, due to an optimal combination of a high precision real-time tomographic ionospheric model, with the geodetic model (see for example Hernandez-Pajares et al. 2000). We will show that a new and simple real-time modelling of MSTIDs doubles the WARTK service area over Europe. WARTK can be applied for both GPS and the new Galileo and GPS modernized systems, and it is being demonstrated in recent and ongoing European projects.

1. Kriging interpolation

The kriging interpolation technique was developed in the field of the geostatistics in the year 1950 by Krige. This is a linear interpolator, see equation (1), in which the kriging technique computes the optimal weight that will be applied in our particular problem.

$$Z_0^* = \sum_{i=1}^{N} \omega_i \cdot Z_i \qquad (1)$$

Where Z_o^* is the value to interpolate, ω_i is the weight to be applied to the sample data Z_i.

The main feature of this interpolation technique is that it can take into account the spatial correlation among the data used in the interpolation process by using the semivariogram (γ_{ij}) function, see equation (2). Thus, the semivariogram is the function that describes the spatial correlation among the data as a function of the distance.

In order to compute the weights applied to the data, the kriging equations has to be solved. In this work the ordinary kriging equations have been applied, which can be written as:

$$\sum_i \omega_i \gamma_{ij} + \lambda = \gamma_{i0} \tag{2}$$

Where ω_i is the weight to be applied to the sample data, γ_{ij} is the semivariogram at the given points and γ_{io} is the semivariogram at the unknown points

In order to apply the ordinary kriging equation the mean values and standard deviation of the data should be independent of the location in order to assure the convergence of the method.

1.1 How to apply kriging to GIM estimation?

As has been explained above in order to apply the ordinary kriging equations, the data has to fulfil certain mathematical requirements. In this context, the ionospheric data is not independent of the location; it has strong dependence in latitude and longitude. Thus, in order to overcome this problem, a base model has to be chosen to compute the residuals between the ionospheric data and the model. In the beginning, different kind of models had been selected. More concretely, a geometrical model (Planar fit), a Climatological model (IRI) and a GPS data driven model (UPC GIM) had been used in order to compute a kriging GIM, and then these GIMs were tested with ionospheric altimeter data in order to check its performance. The model that behaved better, as it could be expected, was the GPS data driven model, which will be the base model to compute all the Kriging UPC GIM.

1.2 Results

The test of the performance of the UPC kriging GIM has been done by means of comparing with:

- Direct VTEC values provided by altimeter data.
- Direct STEC variation information in a given sub-set of receivers (Self-consistency test).
- Double differenced STEC ($\nabla\Delta$STEC) computed with WARTK in post-processing mode.

Indeed, one of the posibilities to compute the performance of the UPC kriging GIM is using the ionospheric data provided by the dual frequency altimeter satellites, TOPEX and JASON. These two satellites are orbiting at a mean height orbit of 1330 km above the Earth's surface, providing their estimation only over the oceans and seas. This characteristic makes the comparison be carried out where the estimations of the GIMs are the worst; this is due to the poor GPS data coverage over the oceans (see Figure 1). Thus, in this way the real capability of the interpolation scheme to compute the ionospheric data is tested.

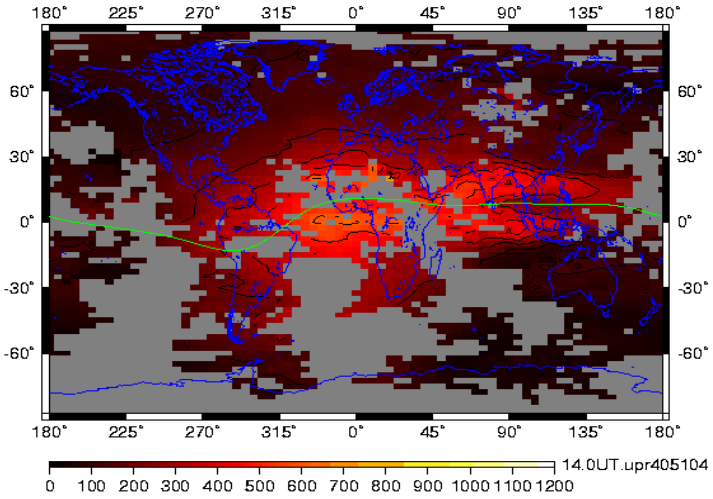

Figure 1: Raw GIM map where it can be seen the data gaps, these are specially important in the equator and South hemisphere (source: UPC, day 51 2004, 14UT).

The test with TOPEX data has been carried out during the year 2002, using more than 1,200,000 observations. This period of time is especially interesting because there is a Maximum on the Solar Cycle. The results show a global improvement over the UPC GIM of about 6%, see next table.

(in TECU)	**BIAS**	**RMS**
UPC	1.8	5.6
UPC kri.	1.8	5.3
IGS	0.3	5.5

Table 1: Global performace of UPC kriging GIM compared with the current UPC GIM and the official IGS GIM regarding to TOPEX VTEC data for the year 2002 with 1,248,020 observations.

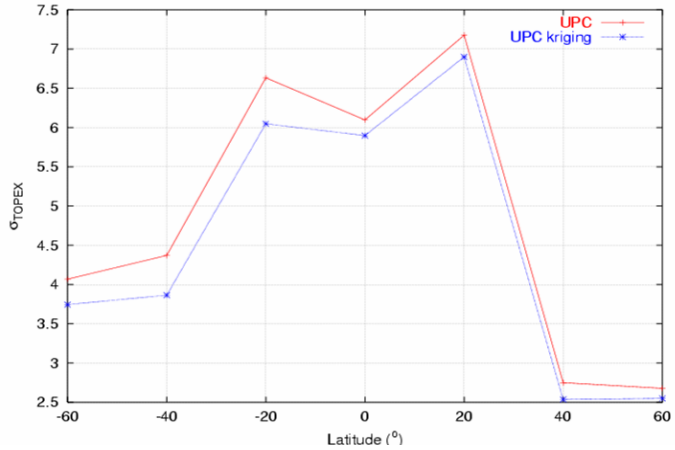

Figure 2: Standard deviation of the UPC and Kriging UPC GIMs regarding to TOPEX data for year 2002, in terms of the latitude.

Another way to show these results is by means of computing the performance over different latitude bands. In this way it can be seen the improvement of the method as a function of the latitude. The results are presented in Figure 2 in which an overall improvement can be seen for all latitude bands. Moreover, the major improvements, of about 9%~11%, are located in the south hemisphere.

When the JASON data is used, the global improvement is less than with TOPEX data, see table 2. This is due to the fact that the period of time is the year 2004, which period is middle – low solar activity.

(in TECU)	**BIAS**	**RMS**
UPC	0.7	3.6
UPC kri.	0.7	3.5
IGS	0.1	3.6

Table 2: Global performance of UPC kriging GIM compared with the current UPC GIM and the official IGS GIM regarding to JASON VTEC data for the year 2004 with 6,455,801 observations.

In this case, a period of high geomagnetic activity has also been studied in order to test the capability of the kriging technique with high ionospheric activity; in the period of time studied the Kp index reaches values greater than 7. In this period of time, more concretely between the day of the year 200 and 220, the maximum Kp index value is 9, this corresponds to the maximum improvement (about 14%, see Figure 3).

Another way to calibrate the UPC kriging GIM is the self-consistency test. It uses the GPS data to show the capability of the GIMs to compute the STEC variation, see Orus et al 2005. This test is used in order to compute the weights that are applied to the weekly combination of the GIM in order to compute the IGS GIMs. In this case, a period of time of 100 days, starting on day 150, 2004, has been studied. The results (see Figure 4) show an improvement of about 16% for the whole period, which points out the smoothness of the estimation with the kriging technique.

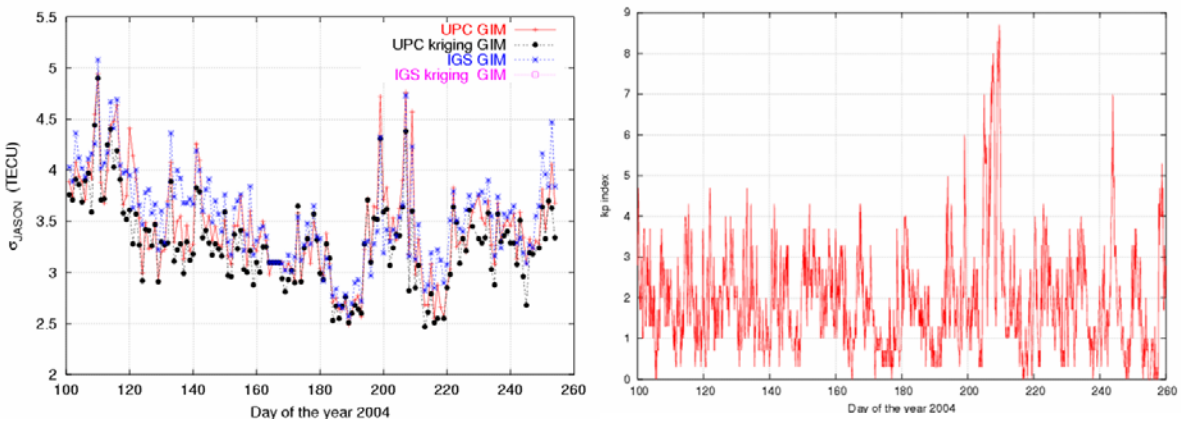

Figure 3: In the right panel the standard deviation of the UPC and IGS GIMs, regarding to JASON VTEC, is depicted. In the left the Kp index for the same period of time of the year 2004 is represented.

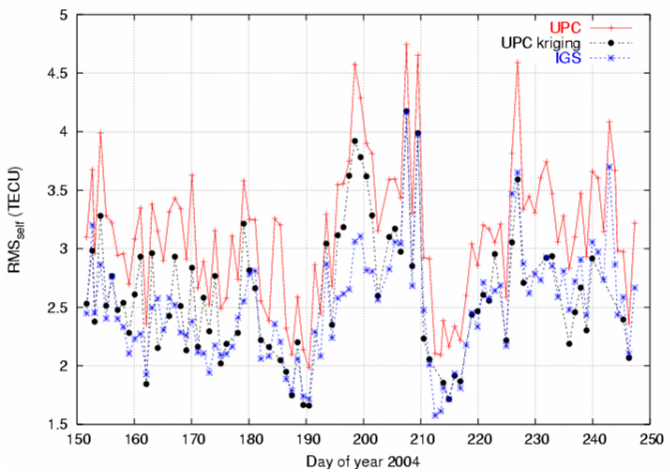

Figure 4: RMS of the UPC, UPC kriging and IGS GIMs regarding to self-consistency test for year 2004.

The last test used to measure the kriging GIM performance is the comparison with double-differenced STEC (∇ΔSTEC) computed with the WARTK technique (see below). As it is known these double differences are very precise since they are computed after computing the carrier phase ambiguities. Thus, in this work a set of stations have been used in Hawaii islands, with baselines ranging from 50 km to 500 km (Figure 5). With this set of station the performance of the ∇ΔSTEC can be computed as function of the distance, in a specially difficult scenario (centered at 20^o of latitude, directly below the Northern Appleton anomaly). In this test the improvements range from shortest baseline, improvement of about 56%, up to about 20% for the longest ones, showing that the UPC kriging GIM has a performance mostly equal to the combined IGS GIM (see again Figure 5).

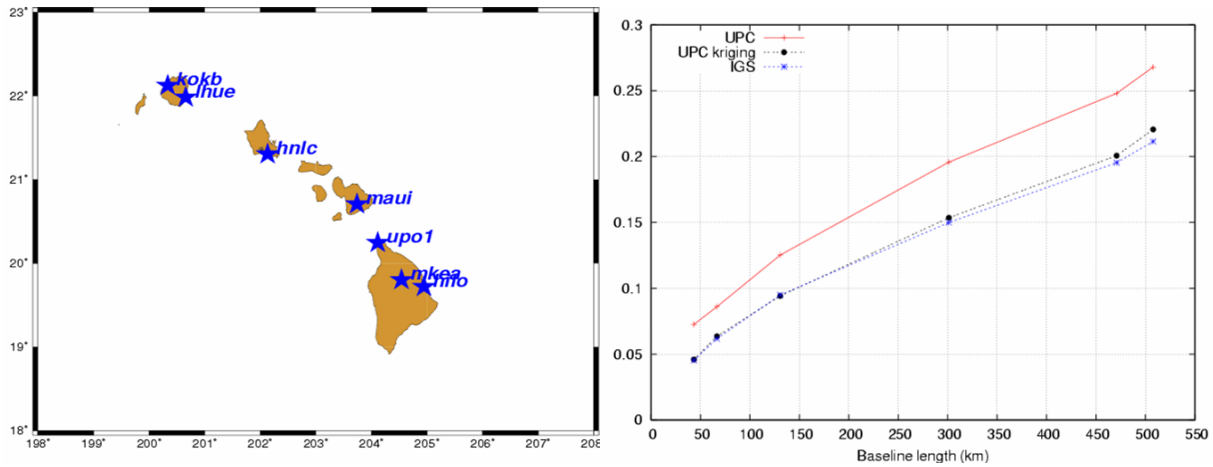

Figure 5. In the left panel there is depicted a map of the stations used for the ∇ΔSTEC test, where MKEA receiver is the reference station for the double differences. In the right panel there is depicted the RMS values of the test for the year 2004.

2. WARTK: subdecimeter-error navigation at hundreds km away

The ionospheric refraction (see exemple in Figure 6) typically limits the real-time ambiguity fixing (and the corresponding navigation with sub-decimeter errors) to baselines of few tens of

km in different approaches in both two and three-frequency systems (RTK, LAMBDA, TCAR, CIR, ITCAR, FMCAR). Wide Area RTK (WARTK) overcomes this problem incorporating an accurate real-time ionospheric model: (1) in two-frequency systems (GPS: WARTK), and (2) in three-frequency systems (Galileo and Modernized GPS: WARTK-3), which allows the extension of the Local Area Galileo services to continental scales (Figure 7). Both approaches (WARTK and WARTK-3) were presented in previous papers and demonstrated in many experiments including a real-time ionospheric prototype (Hernández-Pajares et al. 2000, 2002, 2003).

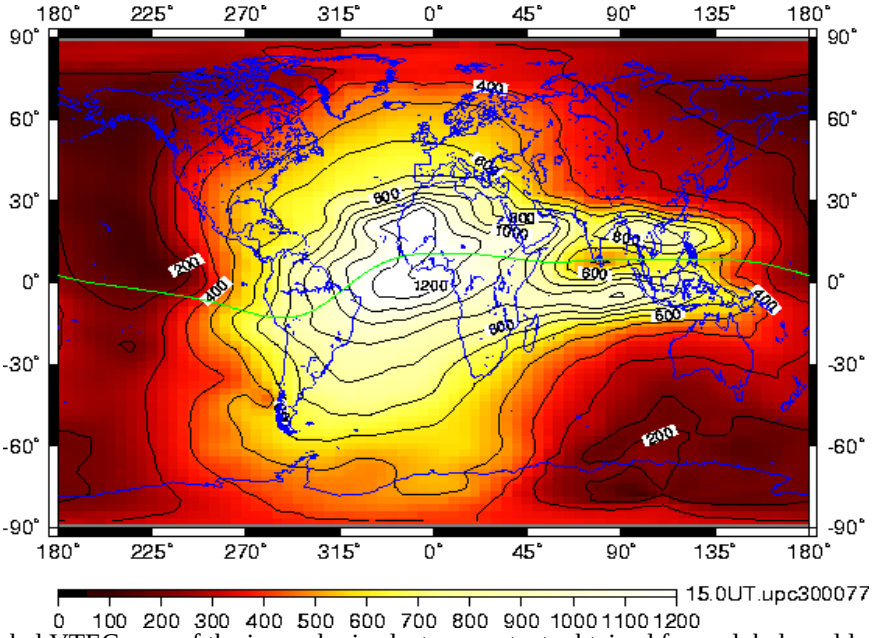

Figure 6: Global VTEC map of the ionospheric electron content, obtained from global worldwide network in Solar Max. conditions (source UPC, day 077, 2000, units: tenths of TECU).

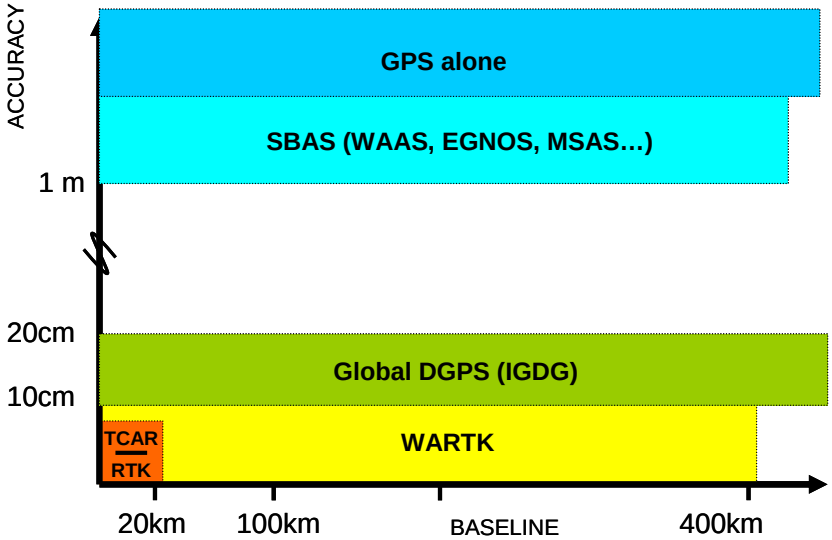

Figure 7: Typical accuracy vs. baseline plot, in which is shown the gap occupied by WARTK (extension of centimetre-level accuracy to hundreds of kilometres far from the nearest reference site).

2.1 The real-time ionospheric model

The ionospheric electron density distribution is decomposed in voxels (see Figure 8 and equation (3) below, solved by continuous Kalman filtering) in the GNSS data driven real-time model. Both models, ionospheric and geodetic, are combined continuosly in a forward filter running in real-time, improving the estimation and fixing of L1, L2 carrier phase ambiguities (Figure 9). From the unambiguous L1-L2, an accurate double differenced STEC (~0.1 TECU) can be obtained and broadcast to the users.

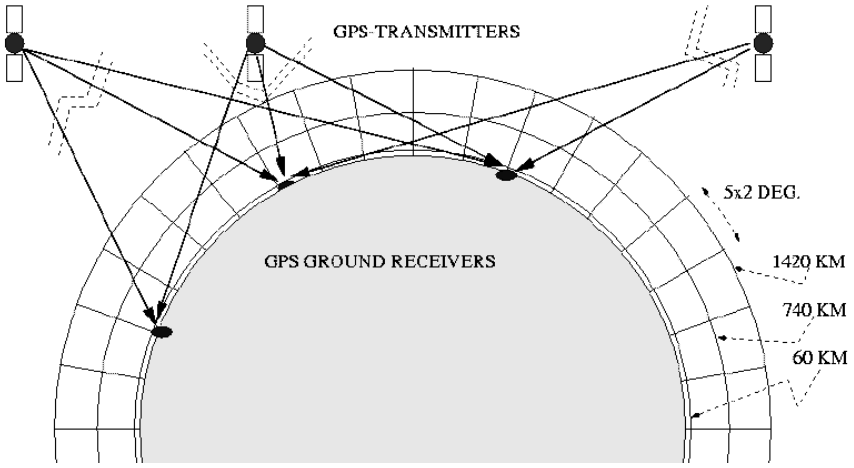

Figure 8: Layout of the tomographic ionospheric model used to estimate the ionospheric electron content in real-time.

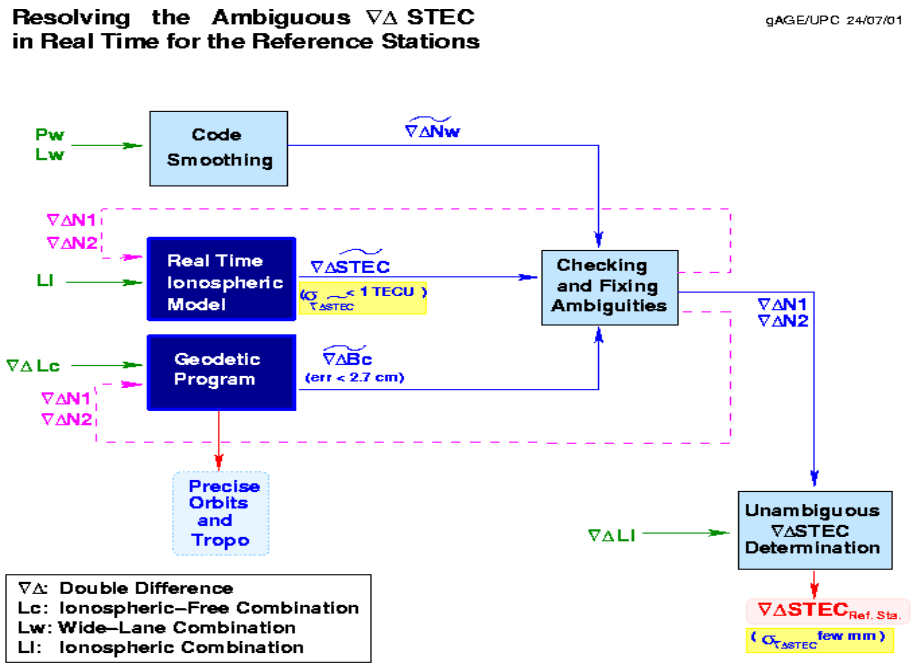

Figure 9: Layout representing the core of the WARTK Processing Facility core.

$$L_I = STEC + B_I = \int_{REC}^{SAT} N_e dl + B_I = \sum_i \sum_j \sum_k (N_e)_{i,j,k} \Delta s_{i,j,k} + B_I \quad (3)$$

2.2 WARTK-EGAL: Service area improvement

One of the main ionospheric effects, when we consider ambiguity fixing associated to precise GNSS navigation, is the so called Travelling Ionospheric Disturbances (TIDs). These ionospheric waves are the main responsibles of the non-linear behaviour of the ionosphere, affecting seriously the user ionospheric interpolation (see a complete study in Hernández-Pajares et al. 2006). Using a simple real-time MSTID model, which takes into account its climatological behaviour, the WARTK service area is doubled (up to 250 km), regarding to a simple MSTID downweighting of MSTID-affected satellites (up to 190 km), and is four times regarding to using just a simple planar fit of slant ionospheric corrections per satellite (~125 km). More details can be seen in Figure 11 and Figure 12 corresponding to permanent and roving receivers represented in Figure 10, in the context of an experiment performed in the WARTK-EGAL Galileo Joint Undertaking project).

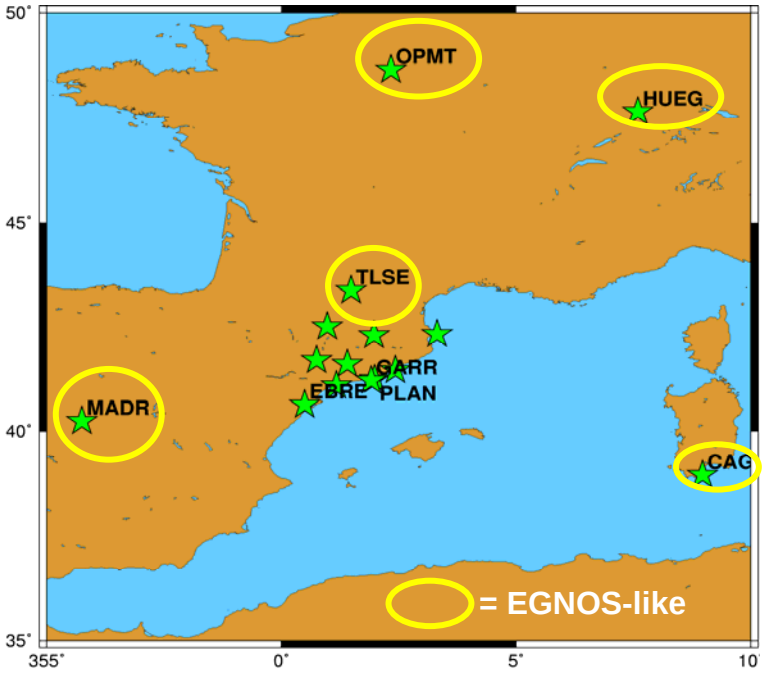

Figure 10: Reference GPS receivers (yellow circles) and static receivers treated as roving ones (green stars), used in one recent WARTK experiment, which results are summarized in the two following figures.

Conclusions

Several conclusions can be extracted for the presented study of ionospheric determination improvement in both global VTEC mapping and accurate STEC navigation:

1) The Kriging algorithm has been adapted to the problem of interpolation in the Global VTEC map generation, behaving better than previous technique.
2) The UPC GIMs improvements due to the kriging are especially important in south hemisphere (few data available), low latitudes (high TEC gradients), Solar Maximum

conditions, reaching up to 11% of improvement, and high geomagnetic activity (14% of improvement).

3) Such improvements are also extended to the potential use of GIMs to predict double differences of ionospheric corrections for geodetic applications.
4) Enhancement of EGNOS/Galileo service is feasible over Europe: from meter-level to centimeter-level accuracy with WARTK, specially considering both tomographic and MSTID modelling.
5)

Acknowledgments

The authors acknowledge to the International GPS Service and JPL the availability of the ground GPS and TOPEX/JASON data sets respectively. This work has been partially supported by the Spanish project ESP-2004-05682-C02-01 and by the Galileo JU WARTK-EGAL project.

References

Hernández-Pajares, M., J.M. Juan, J. Sanz and O.L. Colombo, Application of ionospheric tomography to real-time GPS carrier-phase ambiguities resolution, at scales of 400-1000 km, and with high geomagnetic activity, Geophysical Research L., 27, 2009-2012, 2000.

Hernández-Pajares, M., J.M. Juan, J. Sanz, O.L. Colombo, Improving the real-time ionospheric determination from GPS sites at Very Long Distances over the Equator, J. of Geophysical Res., V.107, No.A10, 1296, 2002.

Hernández-Pajares, M., J.M. Juan, J. Sanz, O.L. Colombo, Feasibility of Wide-Area Subdecimeter Navigation with GALILEO and Modernized GPS, IEEE Trans. on Geoscience and Remote Sensing, V.41, No.9, 2003.

Hernández-Pajares, M., J.M. Juan, J. Sanz, Medium scale Traveling Disturbances affecting GPS measurements: Spatial and temporal analysis, J. of Geophysical Res., Vol..111, A07S11, doi:10.1029/2005JA011474, 2006

Orús, R., Hernández-Pajares, M., J.M. Juan, J. Sanz, Improvement of global ionospheric VTEC maps by using kriging interpolation technique, Journal of Atmospheric and Solar-Terrestrial Physics, doi:10.1016/j.jastp.2005.07.017, 2005.

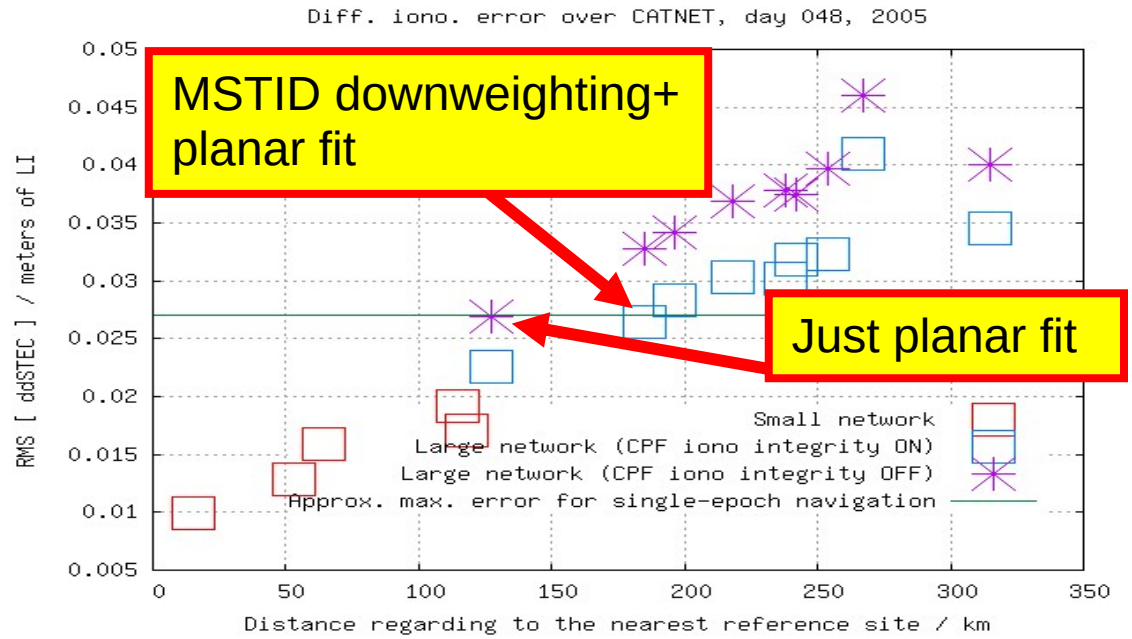

Figure 11: Performance of different ionospheric interpolation procedures for roving users, developed by the authors in previous works (the 0.27 cm line indicates an approximately ionospheric threshold to be able to fix ambiguities in single epoch mode).

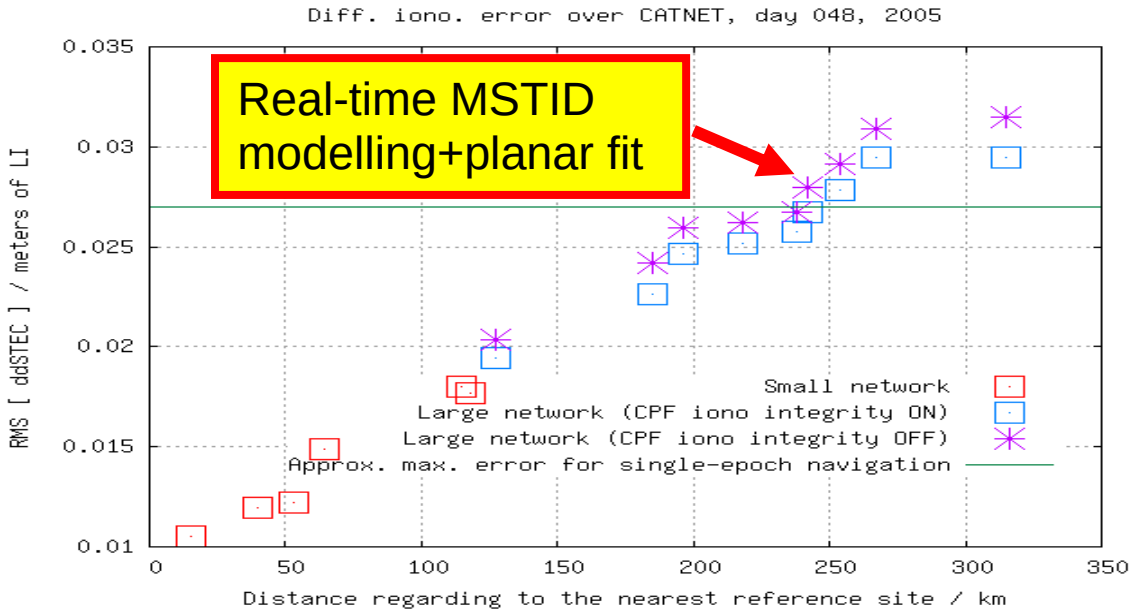

Figure 12: Performance of a new ionospheric interpolation procedures for roving users, taking into account a real-time MSTID model (under patent). The 0.27 cm line indicates an approximately ionospheric threshold to be able to fix ambiguities in single epoch mode.